Manufacturing of Ti–6Al–4V Micro-Implantable Parts Using Hybrid Selective Laser Melting and Micro-Electrical Discharge Machining

Hassanin, Hany; Modica,, Francesco; El-Sayed, Mahmoud; Liu, Jian ; Essa, Khamis

DOI:
10.1002/adem.201600172

DOI: 10.1002/((please add manuscript number))
Article type: Communication

Title
Manufacturing of Ti-6Al-4V Micro-Implantable Parts using Hybrid Selective Laser Melting and Micro-electrical Discharge Machining

Hany Hassanin 1, Francesco Modica 2, Mahmoud Ahmed El-Sayed 3, Jian Liu 4, Khamis Essa5

1 School of Mechanical and Automotive Engineering, Kingston University, London SW15 3DW
2 ITIA-CNR, Institute of Industrial Technologies and Automation, Bari, Italy
3 Department of Industrial and Management Engineering, Arab Academy for Science and Technology and Maritime Transport, Abu Qir, PO Box 1029, Alexandria 21599, Egypt
4 School of Manufacturing Science and Engineering, Sichuan University, Chengdu, China, 610065
5 School of Mechanical Engineering, The University of Birmingham, Edgbaston B15 2TT

Keywords: Selective laser melting, micro-component, micro-electrical discharge machining

The advent in micro/nano electromechanical systems (MEMS/NEMS) has been the main thrust for the advancement of high performance miniaturized systems. In addition, the application of micro manufacturing technologies to biomedical engineering has presented a novel generation of small devices that helped in both medical research and treatment [1-6]. For example; lab on a chip and micro-implant systems allowed the reduction in power consumption, electronic noise and system complexity and capability. However, the materials used in these systems must be biocompatible and able to work in vivo. Popular examples of biocompatible materials include silicon, polymers and glass. Many biocompatible metals have been also used in micro-implants such as titanium alloys, nitinol, platinum and stainless steel [7, 8]. A remarkable advantage of metals over silicon based materials and ceramics is their high strength, eliminating the chance of encountering a failure during service. They also showed outstanding stability in vivo and good impermeability. Therefore, they have been the main choice of hermetic seals of large biomedical implants such as pacemakers [9, 10].

Soft lithography, micro electroforming, and micro gel casting are techniques used to manufacture metal micro-parts. These techniques have been implemented to produce parts with the desired precision and surface quality [2, 11, 12]. Selective laser melting (SLM) is one of the additive manufacturing techniques in which a 3D product is built layer-by-layer [13-15]. SLM allows more freedom for the Computer Aided Drafting (CAD) designers to enable design and topology optimisation. SLM enables the production of near-net-shape complex parts [16-18]. The use of SLM for the fabrication of micro-components has been seldomly reported. Hagemann et al [19] produced micro actuators from NiTi shape memory alloy which could be used for cochlear implants. In addition, Bultmann et al. [20] utilized the geometric freedom offered by the SLM process to produce hollow micro-struts. 316L stainless steel micro-struts with a diameter ranged from 300-740 μm and of length of 3.5 mm were successfully fabricated. In another research, Sutcliffe and co-authors reported the application of SLM to manufacture micro hierarchical structures with complex geometry which could be used in orthopaedic implants and ultra-light aerospace applications [21]. However, the main challenge of SLM as a micro fabrication tool is how the surface quality and the precision of its products can be improved. The surface roughness of SLM components is greatly affected by three main factors. The first factor is the "stair step" effect, which is the stepped approximation by layers of curves and inclined surfaces. This effect is present as a consequence of the additive deposition and fabrication of layers [22]. The second factor is the "balling" phenomenon that occurs during laser melting. The balling effect limits the SLM resolution because it causes the formation of discontinuous tracks [23]. The third factor is the partially melted particles adhered to the parts. In an attempt to improve the surface quality, Zhang et al [24] used atmospheric plasma spraying (APS) alumina coatings to treat the surfaces of SLM stainless steel parts. The surface roughness (Ra) of the vertical and horizontal surfaces before coating was 28 and 17 μm, respectively. Both surface roughnesses were decreased to 15 μm with the APS treatment. However, it was found that the bonding strength

between the deposited layer and the SLM part was relatively weak, which might affect the serviceability of the component. In another study by Yasa et al. [25], laser re-melting was applied to improve the surface finish of Ti-6Al-4V parts from 15 µm to 2.9 µm. However, for micro systems, better surface finish of a value less than a micron is required, which is suggested in the proposed process to be obtained via micro-Electrical Discharge Machining (µ-EDM) [26].

Micro-Electrical Discharge Machining is a thermo-electric process that uses electrical discharges to erode electrically conductive materials by a series of discrete sparks between the work-piece and the tool electrode, both submerged in a dielectric fluid. The process is quite capable of machining intricate profiles from any electrical conductive material irrespective of its hardness and strength [26, 27]. This work introduces a hybrid micro fabrication technology combines both the design freedom of SLM and the high surface quality of µ-EDM. The aim is to manufacture high quality micro implantable components with the highest density and the best surface finishing. Statistical experimental design using analysis of variance technique was used to determine the significance of SLM process parameters on the amount of porosity and internal defects. Microstructure analysis using image processing was used to calculate the parts porosity. After SLM optimization, the samples were further processed using µ-EDM to improve their surface quality. The effect of changing µ-EDM parameters on the resultant surface roughness was also explored.

Seventeen samples with different parametric combinations were built using Design of Experiment (DoE). In these experiments, the laser power range was 100:200 W, laser scan speed range was 500:3000 mm/s and hatching spacing (Scan spacing / laser track width constant (150 µm)) range was 0.2:0.8. The 17 different parametric combinations along with the measured values of porosity are presented in Table 1.

Figure 1 shows the porosity response surface model with respect to laser power, scan speed and hatch spacing. Interpretation of the results in Figure 1 and Table 1 shows that at constant scan speed and hatch spacing of 1500 mm/s and 0.5, respectively, increasing the laser power from 125 to 175 W can decrease the porosity of a SLM part from 1.2% to 0.4%, see Figure 1 (a). Similar reduction in the porosity level can be obtained by decreasing the scan speed from 2375 to 1125 mm/s, while the laser power and hatch spacing are kept at 150 W and 0.5, respectively, see Figure 1 (b). In addition, it can be clearly seen that the porosity level is very sensitive to the hatch spacing values, see Figure 1 (c). The porosity level was dropped from 1 to 0.55% by increasing the hatch spacing from 0.35 to 0.65, at laser power of 150 W and scan speed of 2375 mm/s. In general, it can be concluded that the porosity level can be decreased by either increasing the laser power or reducing the scan speed and/or the hatch spacing. This means the input energy per unit volume has to be increased to a certain level in order to avoid porosity formation. In addition, it seems that the interaction between the hatch spacing and scan speed is also significant, as shown in Figure 1 (d). At higher hatch spacing, the effect of scan speed on porosity formation is more considerable. Similarly, the influence of the hatching spacing is more significant at higher scan speeds. High density can be achieved using slow laser speed and small hatch spacing. This can consequently result in a material re-melting which eliminates powder/metal splashing and porosity formation. Therefore, energy density should be sufficient to avoid incomplete melting. Increasing the scan speed and hatch spacing and/or a decrease in the laser power can cause incomplete consolidation and a smaller melt pool. This can result in entrapment of the voids among the powder particles under the solidified hatch lines and in turn reduces the overall density of the SLM part. From the results in Table 1, the sample from run number 13 experienced a minimum porosity level of 0.25 %, which was produced using laser settings of 175 W laser power, 1125 mm/s scan speed and 0.35 hatch spacing.

An optimisation study was carried out using Design-Expert Software to obtain the optimum processing parameters at which the highest density of the SLM can be achieved. Since the SLM components were planned to undergo a finishing operation using the µ-EDM, the objective function was set to minimise the porosity. The results are shown in Figure 2 (a) which shows the contour plot for the optimisation function. The model suggested that the optimised values of the process parameters would be 200 W, 1000 mm/s and 0.67 for the laser power, scan speed and hatch spacing, respectively. This is equivalent to an energy density of 100 J/mm^3. Results from the 17 samples shows that the lowest porosity is 0.25%. On the other hand, the process optimisation shows that the predicted optimum porosity level is 0.13%. To examine the predicted process parameters, five identical SLM micro components were fabricated using a laser power of 200 W, a scan speed of 1000 mm/s and a hatch spacing of 0.67. The average measured value of the porosity of the five samples was 0.17%.

Figure 2 (b) shows a plot of the porosity versus the energy density for the data previously provided in Table 1. The figure shows micrographs of samples with different porosity levels at both low and high energy density and a sample from run number 13, which has the minimum porosity (See Table 1). It also shows a micrograph of the sample produced using the predicted conditions. The graph shows that the porosity content consistently decreased with increasing the energy density, which may be due to the improved consolidation of the metal powder, until achieving a minimum value at a range of energy density of about 80 to 100 J/mm^3. However, a further increase in the energy density causes the porosity content to scatter beyond that level until 200 J/mm^3. In this region, other defects such as keyhole formation, which is produced due to vapourisation of the metal powder, might be produced within the SLM part. This type of defects also increases the porosity level. The presence of a threshold for the energy density that gives a maximum material density was reported by previous researches [28-31]. In particular, the energy density required to produce fully dense

components from commercially pure titanium and Ti–6Al–4V powder was estimated to be about 120 J/mm^3 [7]. In the current study, a nearly fully-dense Ti–6Al–4V SLM micro-parts were obtained at relatively lower energy density, perhaps due to the application of an island scanning strategy.

The micro-parts produced by SLM were post processed via μ-wire-EDM in order to improve the surface quality of specific surfaces. The average surface roughness of the SLM components was measured before the machining by the confocal microscope (Zeiss CSM700) to be 14.7 μm. The performance of the EDM process for both the roughing and finishing regimes, and the different parameters adopted for each are summarised in Table 2 and Figure 3.

As expected, the μ-wire-EDM process improved both surface roughness (Ra) and flatness of the SLM parts, see Figure 3. In order to implement the finishing phase, a stock allowance on the nominal dimension should be considered when the part is realized in SLM. A higher allowance is often needed when the surface porosity level is high and/or surface flatness is pour. Figure 3 (a) and (b) shows the scanning of the surface of the square face of the micro component before and after being machined using the μ-wire-EDM. Figure 3 (c) shows an SEM image of the vertical surface topography of the SLM part before micro machining. As shown, the surface roughness of the part is limited by the "balling" phenomenon that occurs during laser melting. Particles stuck on the surface of the part are also contribute to the poor surface quality. Figure 3 (d) shows a confocal acquisition of the micro-components showing the roughing and finishing regimes using the optimum μ-EDM parameters. It can be clearly seen that, the machined surface experienced a good surface finish. However, some rounded edges due to the SLM process can be also observed. The surface roughness (Ra) was around 4.6 μm for the roughing regime and was between 0.6 μm and 0.8 μm for finishing regime, See

Table 2. The improvement in the surface roughness in the finishing regime is due to use of reduced discharge energy, which enabled the production of a small crater size and in turn obtaining an outstanding surface quality. The introduced hybrid process was also applied to different electro-conductive materials such as Fe. Figure 3 (e) and (f) show a comparison between SLM iron micro-gear before and after the µ-EDM machining showing clearly the roughing and finishing regimes. It should be emphasized that the use of µ-EDM to machine micro parts for medical purposes might be of concern. Possible surface contamination by Cu during the machining might affect the behaviour of Ti-6Al-4V components in the human body. Further investigations are necessary to evaluate the influence of µ-EDM on the biocompatibility of different materials.

This research was carried out to cover the gap in producing high precision micro-components using SLM as well as to study the potential of using µ-EDM in the field of additive manufacturing. Selective laser melting process has been optimised to minimise porosity of the micro-parts. It was shown that the porosity can be reduced using the optimum laser process parameters predicted using a design-of-experiments approach. In addition, surface roughness of the SLM micro-components can be significantly improved using µ-EDM technique. It was found that, when the material is electro-conductive, µ-EDM process is a good choice for improving surface roughness and to machine sharp micro-features. In order to get the best results of the proposed technology, the definition of a common reference is required to align the target features. Furthermore, An ad-hoc clamping system is crucial for reducing machining error and improving the final surface roughness and overall machining time. Current limitations of the micro µ-EDM include the inability to machine non-conductive materials, 3D curved surfaces, non-pass through surfaces and the low metal removal rate.

Experimental Section

In this study Ti-6Al-4V gas-atomised powder was supplied by TLS Technik GmbH. The size range was 25–50 µm, as measured using Coulter LS230 laser diffraction particle size analyser. To perform the design of experiment Design-Expert® Software Version 7.0.0 from Stat-Ease was used and the response surface methodology was adopted **[32]**. Design–Expert was applied to generate an experimental design to screen the process input parameters. The software utilised the analysis of variance (ANOVA) technique to determine the statistical significance of these parameters. In order to determine the equations of the response surface, the central composite second order design was used**.** The expression for the second order central composite design is given in Equation 1:

$$Y = b_o + \sum b_i x_i + \sum b_{ii} x_i^2 + \sum b_{ij} x_i x_j \quad (1)$$

where Y is the process yield (or the response surface), while x_i are the factors or process parameters. The expression contains linear terms in x_i, quadratic terms in x_i^2, and product terms in $x_i x_j$. The terms b_i , b_{ii}, and b_{ij} are constant coefficients. Method of least squares is used to determine the constant coefficients. In this way, the response surface methodology can quantify the relationship between controllable input parameters and the obtained response surface. Finally, the software was used for the optimisation of the process responses. The optimisation involves setting a goal (e.g. maximise or minimise) for each of the responses being studied. The goals are then combined into an overall desirability function. The program seeks to maximise this function. The goal seeking begins at a random starting point and proceeds up the steepest slope to a maximum. In this study, DoE was used to study the effect of SLM process parameter**s** such as laser power, scan speed and hatch spacing on the porosity

of the SLM parts. The optimum process parameters required for obtaining minimum porosity were also predicted.

A Concept Laser M2 powder bed system was used to fabricate the Ti-6Al-4V micro-parts. All samples were built using a layer thickness of 20 µm and the build was carried out under Argon. An "island scanning strategy" was applied to manufacture the SLM samples. To characterise the porosity in the samples, polished surfaces were examined using a Zeiss Axioskop microscope. 20 images were captured for each sample and ImageJ Software was used to determine the area fraction of the pores. After the assessment of the porosity, the parameters setting suggested by the model to produce the minimum porosity was used to fabricate five micro-components with a square cross-section of 3x3 mm and minimum feature of 200 µm. These components were further machined via micro-EDM to enhance their surface quality.

The micro-EDM machine used for the present study was a Sarix SX-200 (SARIX SA, Switzerland), with three translational axes (XYZ) and one rotational axis (C). It is provided with a relaxation type generator enabling the discharge of very fine pulses (discharge energy down to few µJ). The machine is equipped with a wire-EDM unit (SX-Arianne), which uses a brass wire of 0.2 mm diameter capable of shaping micro-features. Positive polarity was applied through the entire cutting operation, and hydrocarbon oil was used as dielectric. The machining of the sample was performed using two sets of parameters; for roughing and finishing regimes, as described in Table 3. An Axio CSM 700 confocal microscope from Carl Zeiss was used to evaluate the overall shape and surface roughness (Ra) of the samples before and after the micro-EDM process.

References

[1] W.M. Zhang, K.M. Hu, Z.K. Peng, G. Meng, Sensors (Switzerland) 15 (2015) 26478-26566.
[2] H. Hassanin, H. Ostadi, K. Jiang, International Journal of Advanced Manufacturing Technology 67 (2013) 2293-2300.
[3] A. Cobo, R. Sheybani, E. Meng, Advanced Healthcare Materials 4 (2015) 969-982.
[4] P. Song, D.J.H. Tng, R. Hu, G. Lin, E. Meng, K.-T. Yong, Advanced Healthcare Materials 2 (2013) 1170-1178.
[5] D. Fine, A. Grattoni, R. Goodall, S.S. Bansal, C. Chiappini, S. Hosali, A.L. van de Ven, S. Srinivasan, X. Liu, B. Godin, L. Brousseau, I.K. Yazdi, J. Fernandez-Moure, E. Tasciotti, H.-J. Wu, Y. Hu, S. Klemm, M. Ferrari, Advanced Healthcare Materials 2 (2013) 632-666.
[6] G.H. Lee, J.S. Lee, X. Wang, S. Hoon Lee, Advanced Healthcare Materials 5 (2016) 56-74.
[7] L.C. Zhang, H. Attar, Advanced Engineering Materials 18 (2016) 463-475.
[8] N. Dai, L.-C. Zhang, J. Zhang, Q. Chen, M. Wu, Corrosion Science 102 (2016) 484-489.
[9] N.E. Vrana, A. Dupret-Bories, P. Schultz, C. Debry, D. Vautier, P. Lavalle, Advanced Healthcare Materials 3 (2014) 79-87.
[10] M. Gasik, L. Van Mellaert, D. Pierron, A. Braem, D. Hofmans, E. De Waelheyns, J. Anné, M.-F. Harmand, J. Vleugels, Advanced Healthcare Materials 1 (2012) 117-127.
[11] M. Imbaby, K. Jiang, I. Chang, Journal of Micromechanics and Microengineering 18 (2008).
[12] A. Mohammadkhani, H. Hassanin, C. Anthony, K. Jiang, Microelectronic Engineering 98 (2012) 266-269.
[13] C.H. Lee, Y.J. Kim, J.H. Jang, J.W. Park, Nanotechnology 27 (2016).
[14] A.-V. Do, B. Khorsand, S.M. Geary, A.K. Salem, Advanced Healthcare Materials 4 (2015) 1742-1762.
[15] S.C. Cox, P. Jamshidi, N.M. Eisenstein, M.A. Webber, H. Hassanin, M.M. Attallah, D.E.T. Shepherd, O. Addison, L.M. Grover, Materials Science and Engineering: C 64 (2016) 407-415.
[16] J.S. Hötter, M. Fateri, A. Gebhardt, Selective laser melting of metals: Desktop machines open up new chances even for small companies, Advanced Materials Research, vol 622, 2013, pp. 461-465.
[17] S. Li, H. Hassanin, M.M. Attallah, N.J.E. Adkins, K. Essa, Acta Materialia 105 (2016) 75-83.
[18] C. Qiu, S. Yue, N.J.E. Adkins, M. Ward, H. Hassanin, P.D. Lee, P.J. Withers, M.M. Attallah, Materials Science and Engineering: A 628 (2015) 188-197.
[19] R. Hagemann, C. Noelke, T. Rau, S. Kaierle, L. Overmeyer, V. Wesling, W. Wolkers, Journal of Laser Applications 27 (2015) S29203 (29208 pp.).
[20] J. Bültmann, S. Merkt, C. Hammer, C. Hinke, U. Prahl, Journal of Laser Applications 27 (2015) S29206.
[21] C. Sutcliffe, W. Brooks, W. Cantwell, P. Fox, J.T. Odd, R. Mines, The rapid manufacture of micro hierarchical structures by selective laser melting, 24th International Congress on Applications of Lasers and Electro-Optics, ICALEO 2005, October 31, 2005 - November 3, 2005, Laser Institute of America, Miami, FL, United states, 2005, pp. 1082-1088.
[22] G. Strano, L. Hao, R.M. Everson, K.E. Evans, Journal of Materials Processing Technology 213 (2013) 589-597.
[23] K. Mumtaz, N. Hopkinson, Rapid Prototyping Journal 15 (2009) 96-103.
[24] B. Zhang, L. Zhu, H. Liao, C. Coddet, Applied Surface Science 263 (2012) 777-782.
[25] E. Yasa, J. Deckers, J.P. Kruth, Rapid Prototyping Journal 17 (2011) 312-327.

[26] A.P. Tiwary, B.B. Pradhan, B. Bhattacharyya, The International Journal of Advanced Manufacturing Technology 76 (2015) 151-160.
[27] U. Maradia, M. Scuderi, R. Knaak, M. Boccadoro, I. Beltrami, J. Stirnimann, K. Wegener, Procedia CIRP 6 (2013) 157-162.
[28] B. Vrancken, L. Thijs, J.P. Kruth, J. Van Humbeeck, Journal of Alloys and Compounds 541 (2012) 177-185.
[29] N. Read, W. Wang, K. Essa, M.M. Attallah, Materials and Design 65 (2015) 417-424.
[30] R. Morgan, C.J. Sutcliffe, W. O'Neill, Journal of Materials Science 39 (2004) 1195-1205.
[31] J.P. Kruth, L. Froyen, J. Van Vaerenbergh, P. Mercelis, M. Rombouts, B. Lauwers, Journal of Materials Processing Technology 149 (2004) 616-622.
[32] Y.J. Liu, S.J. Li, H.L. Wang, W.T. Hou, Y.L. Hao, R. Yang, T.B. Sercombe, L.C. Zhang, Acta Materialia 113 (2016) 56-67.

Table 1: Matrix building parameters and porosity content %.

Run	Laser Power (W)	Scan Speed (mm/s)	Hatching Spacing)	Porosity %
1	100	1750	0.5	1.90±0.2
2	125	1125	0.35	0.54±0.05
3	125	1125	0.65	0.51±0.07
4	125	2375	0.35	1.0±0.12
5	125	2375	0.65	2.36±0.22
6	150	500	0.5	0.34±0.05
7	150	1750	0.2	0.76±0.06
8	150	1750	0.5	0.80±0.07
9	150	1750	0.5	0.70±0.06
10	150	1750	0.5	0.69±0.07
11	150	1750	0.8	1.62±0.2
12	150	3000	0.5	2.10±0.3
13	175	1125	0.35	0.25±0.05
14	175	1125	0.65	0.27±0.04
15	175	2375	0.35	0.50±0.06
16	175	2375	0.65	1.35±0.15
17	200	1750	0.5	0.40±0.05

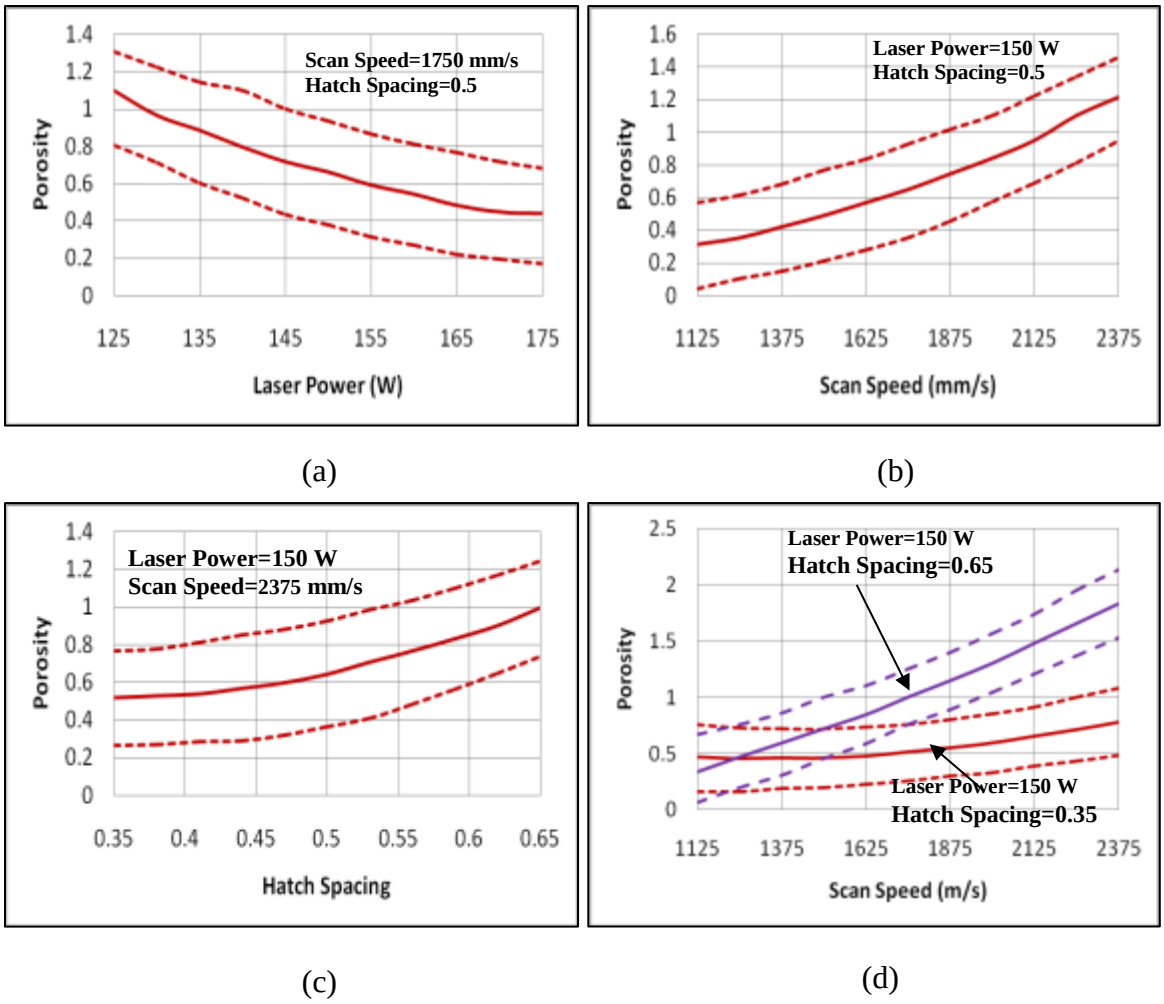

Figure 1: Response surface plot showing the effect of (a) laser power, (b) scan speed, (c) hatch spacing and (d) the interaction between speed and hatch spacing on the porosity %. The solid line represents model prediction.

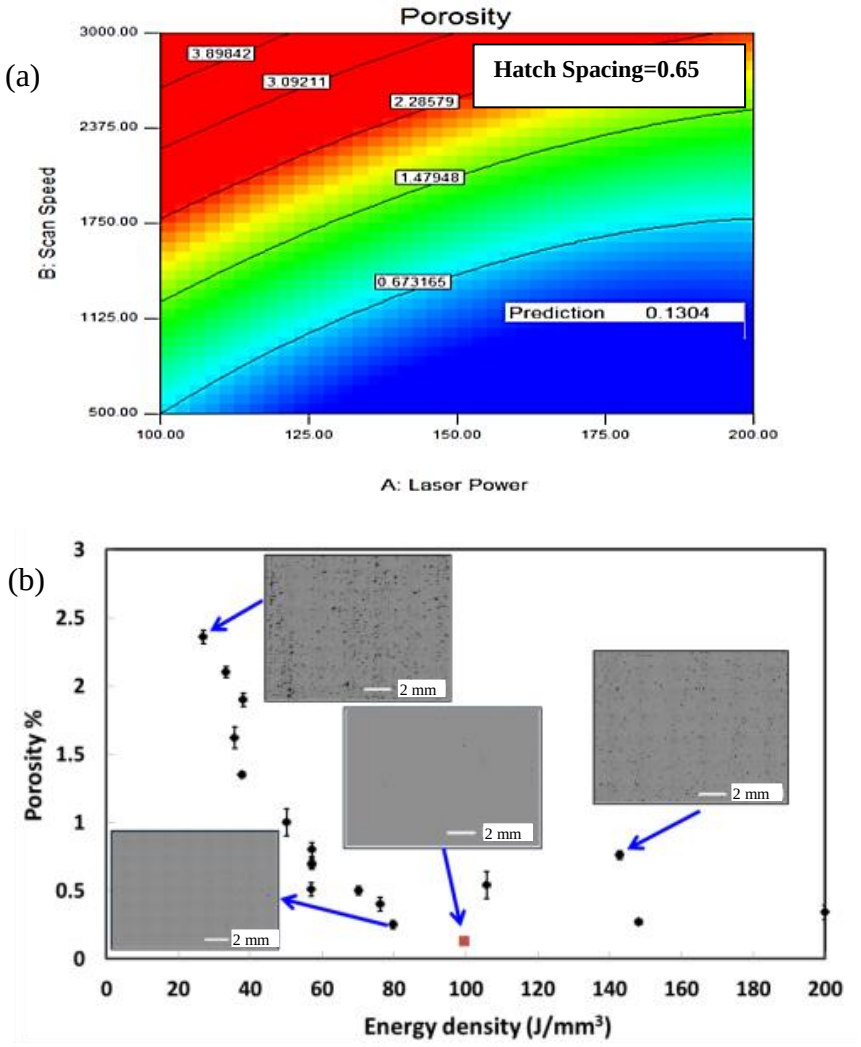

Figure 2: (a) Predicted optimum laser power and scan speed for minimum porosity %, (b) Porosity % variation versus the energy density. (Black is DoE samples and Red is the optimised sample).

Table 2: Wire EDM process performance

Machining Regime	Step-over	Stripe width (mm)	Gain	Average speed (mm/min)	Ra (µm)
Original	-	-	-	-	14.7
Roughing	0.1 mm / 50%	3	10	0.68	4.6
	0.2 mm / 100%	3	20	1.029	
Finishing	0.025 mm / 12.5%	3	10	0.463	0.8
	0.01 mm/ 5%	3	10	0.796	
	0.01 mm/ 5%	1.5	10	1.682	

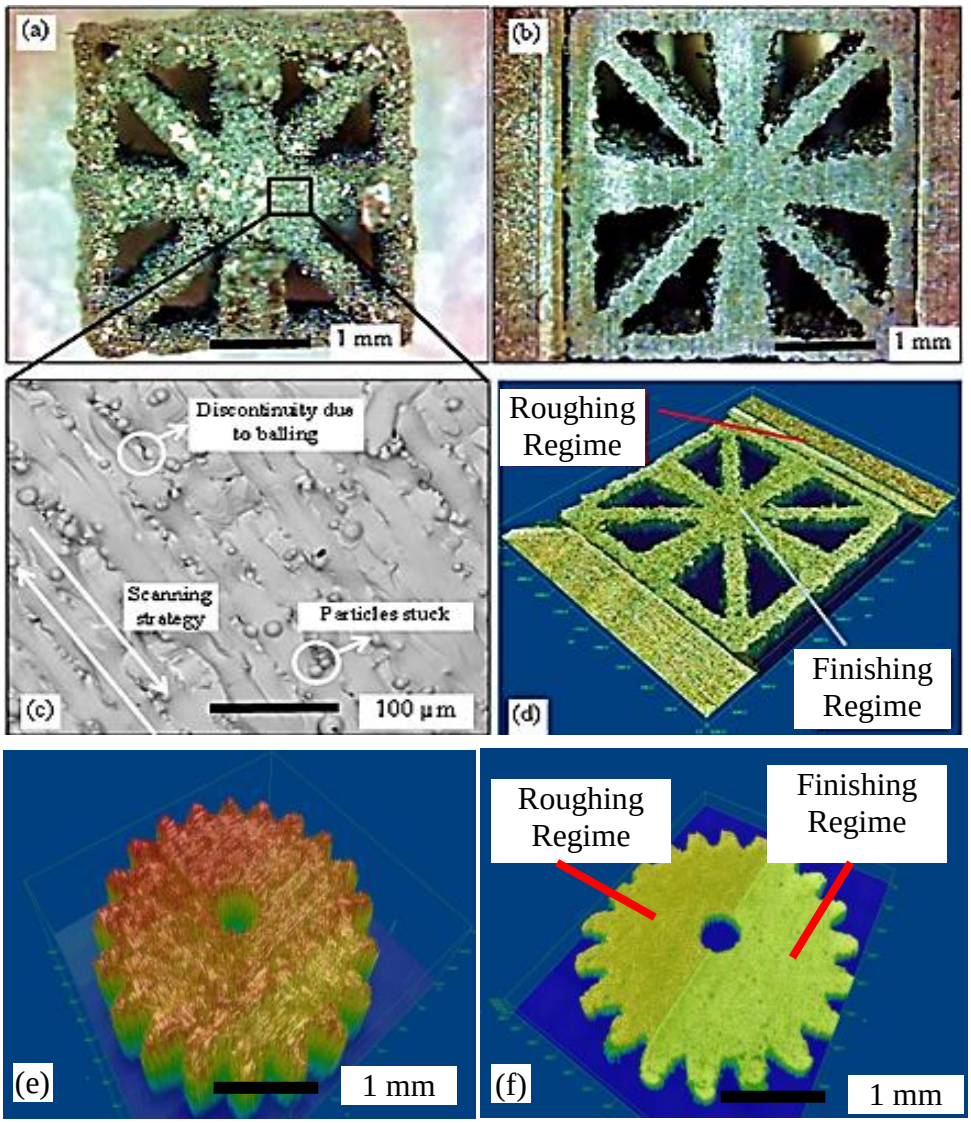

Figure 3: Optical micrographs of the micro-component surface before (a) and after (b) the µ-EDM machining, (c) SEM image of the as SLM vertical surface (d) Confocal acquisition of the micro-components showing the roughing and finishing regimes (e) Confocal acquisition of the as SLM Fe micro-components, (f) as µ-EDM micro-gear

Table 3: Technological parameters adopted in wire-EDM machining for roughing and finishing regimes

Regime		Roughing	Finishing
Electrode Polarity	+/-	+	+
Width	[µs]	5	4.5
Freq	[kHz]	110	180
Current	[index]	70	80
Voltage	[V]	110	130
Gap	[index]	65	75
Energy	[index]	365	105
Wire Diameter	[mm]	0.2	0.2
Working Diameter	[mm]	0.22	0.21